J. Mater. Environ. Sci. 3 (6) (2012) 1147-1152 *Azib et al.*
ISSN : 2028-2508
CODEN: JMESCN

Structural, microstructural and optical characterization of polyol-mediated ZnS/PVP nanocomposite powders and films

T. Azib[1], H. Labiadh[2], M. Gaceur[1], D. Montero[1], S. Ammar[1], L. Smiri[2], T. Ben Chaabane [2,*]

[1] *ITODYS, Université Paris Diderot – Paris 7, UMR-CNRS 7086, 15 Rue Jean de Baïf, 75205 Paris, France.*
[2] *Unité de Recherche UR 12-30 Chimie Inorganique et Structurale, Faculté des Sciences de Bizerte, 7021 Jarzouna, Tunisie.*

Received 17 Feb 2012, Revised 28 July 2012, Accepted 28 July 2012
[*]Corresponding author:, e-mail : Taharbch@yahoo.com , *Fax*: 00 216 72 59 15 66.

Abstract
Poly-N-vinyl-2-pyrrolidone (PVP) capped ZnS nanoparticles were prepared by the so-called polyol process starting from zinc acetate salt, thiourea and PVP_{40} polymer in diethyleneglycol. Dense nanocrystalline ZnS/PVP composite films were elaborated by spray pyrolysis on a moderately heated glass substrate, using a polyol-mediated sol. X-Ray Diffraction (XRD) and Transmission Electron Microscopy (TEM) confirmed the formation of cubic ZnS phase as nanocrystals into the polymer matrix. Optical analysis based on Kubelka-Munk method of the recorded absorption UV-Visible spectra of the films showed an enhancement of the gap value compared to that of the bulk material. This enhancement is discussed in relation with the crystal size of the semiconductor and its dispersion in the polymer matrix.

Keywords: ZnS nanocrystals, polyol process, nanocomposite film, spray coating, optical properties

Résumé : Des nanoparticules de ZnS enrobées par le poly-N-vinyl-2-pyrrolidone (PVP) ont été préparées par la méthode dite d'hydrolyse forcée en milieu polyol à partir des précurseurs : acétate de zinc, thiourée et le polymère PVP_{40}. Le diethylène glycol est utilisé comme solvant. Des films de composites ZnS/PVP ont été élaborés à partir de sols pulvérisés sur des substrats en verre modérément chauffés. Les analyses par Diffraction des Rayons X (DRX) et par Microscopie en Transmission (TEM) confirment la formation de nanocristaux de ZnS de phase cubique dans la matrice polymère. Le traitement des spectres d'absorption UV-Visible des films par la méthode de Kubelka-Munk montre une augmentation de l'énergie du gap comparée à celle du composé massif. Cette augmentation est discutée en fonction de la taille des nanocristaux de semi-conducteur et de leur dispersion dans la matrice polymère.

Mots Clès : Nanocristaux de ZnS, voie polyol, film de nanocomposite, pulvérisation, propriétés optiques.

1. Introduction
Many research activities have been devoted to the synthesis and characterization of semiconductor nanoparticles called quantum dots (QDs). This interest is due to their size-related physical properties [1]. Consequently, the QDs were highly studied for their electric and optical properties [2,3,4,5].Among the various QDs materials, ZnS is an important II-VI semiconductor with a direct wide band gap (for the bulk cubic phase, Eg = 3.66 eV [6,7]), exhibiting a high index of refraction and a large transmittance in the visible range.

Since the inherent crystallinity of ZnS nanoparticles and their regular morphology with almost uniform size distribution play an important role in their physical properties, their preparation conditions must be strictly controlled. In that respect, the polyol method has proved efficient with regard to the synthesis of nanoscaled inorganic materials in general and chalcogenide ones in particular [8,9,10].

For oxides preparation, polyols appear to be very powerfull media. Their high boiling point, namely 245°C for diethyleneglycol, permits performing syntheses at temperature generally higher than that used in classical sol-gel method. The obtained oxide particles very often exhibit a high crystalline quality [11,12]. Moreover, the polyols act as surfactants.

The chelation of the solid nuclei by polyol molecules, during the solid formation, may limit the particle growth and prevent their agglomeration. Unfortunately, in the case of sulfide preparation, the polyols don't wholly play this role, because oxidation reactions in these media are possible and S-S bridges can be formed between sulfide particles leading to their strong aggregation. Such phenomenon was already observed for other synthetic routes. Aggregated nanocrystalline ZnS semiconductors have been produced by sulfate salts calcination method [13],solvothermal route [14,15,16], ball-milling [17] etc. Dispersing agents, such polyvinylpyrrolidone (PVP), were proposed as additives to avoid the aggregation. For instance, ZnS/PVP nanocomposite powders were produced by a microwave route in N,N-dimethylformamide solvent [18] as well as by a co-precipitation method in aqueous [19] or non-aqueous [20] solvent. Composite films were also prepared by sol-gel coating techniques [21,22].

In an another point of view, the combination of inorganic nanoparticles and polymers, such as PVP, in a solid composite form provides stable and processable material integrating the promising properties of both components. Moreover, polymers possess flexible reprocessability which can be attractive for optical or opto-electronic devices.

So for all these reasons, we purpose in the present work to prepare nanometer scaled ZnS particles using the polyol process in presence of PVP. In a first time, the produced polyol-based sol is used as spraying solution to coat a moderately heated glass substrate to form a dense, continuous and thin composite film. In parallel, the formed polymer capped semiconductor particles in the polyol are recovered by centrifugation to obtain a composite powder. The structural, microstructural and optical properties of the produced materials are discussed in relation with the size and the aggregation state of the ZnS particles.

2. Experimental Procedure

2.1. Preparation

The ZnS/PVP product was obtained as powder, polyol-mediated sol and glass supported film. For comparison, pure ZnS product was also prepared using the same protocol without adding PVP. All the reagents and solvent were purchased from ACROS and used without further purification.

Composite powder was prepared by mixing 4.54 g of zinc acetate salt ($Zn(CH_3CO_2)_2.2H_2O$), 1.88 g of thiourea ($S(NH_2)_2$) and 1.33 g of Poly(N-vinyl-2-pyrrolidone) polymer of 40000 DA molecular weight (PVP_{40}) in 100 mL of diethyleneglycol (DEG). The nominal atomic PVP_{40}/Zn^{2+} ratio was fixed to $3.3\ 10^{-3}$. The mixture was heated for 40 min at 180 °C under vigorous mechanical stirring. After cooling to room temperature a white powder was recovered by centrifugation. It was twice re-suspended in ethanol and again centrifuged, in order to remove polyol residue. The powder was then dried in air at 50°C.

Sol was prepared by dividing the nominal reagents concentrations by a factor 100. The polyol-based colloidal solution was stable and no powder was recovered by centrifugation.

Film was obtained by diluting the previously prepared sol with ethanol in appropriated volumic ratio and spraying continuously the mixture onto a 25×25×1 mm^3 glass substrate moderately heated (200°C) during about 3s, using a home-made apparatus [23]. The spraying conditions were already described in a previous work [23]

2.2. Characterization techniques

The identification of the crystal structure was carried out by X-ray diffraction using a X'pert Pro diffractometer (Panalytical) equipped with a Co X-ray tube (λ = 1.7889 Å) in the 2θ range 20-80°. The microstructure of the powder and sol was determined by Transmission Electron Microscopy (TEM) using a Jeol-100 CX II microscope operating at 100 kV, and that of the film was characterized by scanning electronic microscope (SEM) using a JEOL-JSM 6100 microscope operating at 35 kV. The chemical composition of the samples was checked using an energy dispersive spectrometer (EDX) mounted on the SEM microscope.

UV-Visible diffuse reflectance spectra of the powder and films were recorded on a Cary Varian 5E spectrophotometer equipped with a PTFE-coated integration sphere. The optical absorption spectra of the sols were measured in a transmission mode on the same spectrophotometer using a quartz tube.

3. Results and discussion

3.1. Structural and microstructural results

The XRD patterns of the obtained powders ZnS and ZnS/PVP powders and film are given in Figure 1.

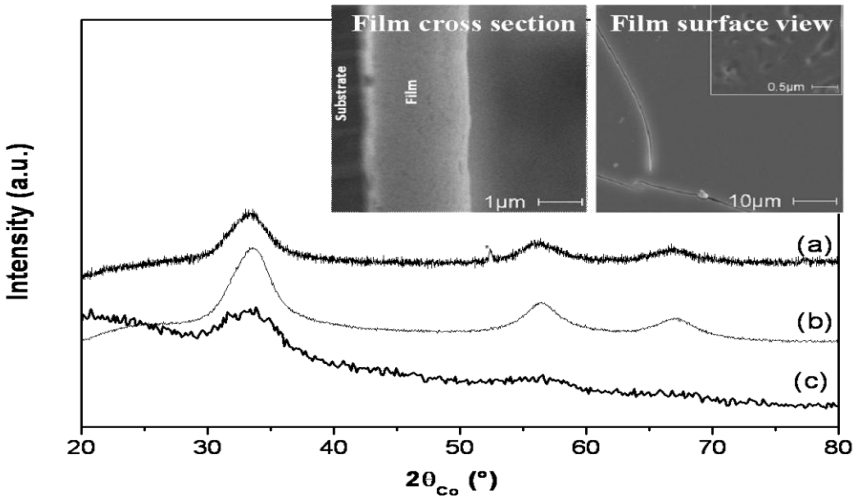

Figure 1. XRD patterns of the as-produced ZnS (a), ZnS/PVP (b) powders and ZnS/PVP film (c). Note (*) corresponds to the diffraction of the sample holder. SEM images of the cross-section and surface view the as-deposed ZnS/PVP film are given in the inset.

In all the cases, the diffraction peaks are matching perfectly with the (111), (220) and (311) crystalline planes of the cubic ZnS phase. No characteristic peak of foreign phase was detected. The calculated lattice constant "*a*" was determined using the Fullprof software [24] based on the Rietveld method. The fitted *a* value, 5.36 Å, is found to be closed to that of cubic ZnS bulk *a* = 5.34 Å (JCPDS card N° 80-0020). The peak broadening in the XRD patterns clearly indicated the formation of very fine crystals. The crystallite size, inferred from the XRD peak width using MAUD software [25] which is also based on the Rietveld method, is found to be about 3 nm for the powders and 2 nm for the films (Table 1). The size difference is mainly due to the reagent concentration difference (a factor 100).

EDX analysis confirmed also the formation of ZnS phase since an equal amount of Zn and S atoms is measured in both ZnS and ZnS/PVP preparations. In the latter case, large amounts of carbon and nitrogen are measured in agreement with the formation of composite materials.

Table 1. Main microstructural and optical characteristics, including the calculated QD radius R, of the studied ZnS and ZnS/PVP sols, powders and films.

	$<L_{XRD}>$ nm	$<D_{TEM}>$ nm	Eg / eV	R (*) nm	R (**) nm	R (***) nm	R (****) nm
ZnS bulk	-	-	3.66	-	-	-	-
ZnS sol	-	1.7±0.6	3.97	1.88	2.34	2.91	2.54
ZnS/PVP sol	-	2.0±0.3	3.97	1.88	2.34	2.91	2.54
ZnS powder	2.8	-	3.71	3.56	4.43	5.50	4.81
ZnS/PVP powder	2.9	-	3.89	2.14	2.60	3.30	2.91
ZnS/PVP film	2.2	-	4.00	1.81	2.20	2.70	2.44

(*) μ = 0.31 [30] ; (**) μ = 0.20 [20] ; (***) μ = 0.13 [32] ; (****) μ = 0.17 [33]

To assess the size and microstructure of the produced materials, drops of suspensions of the ZnS and ZnS/PVP powders dispersed by sonication in ethanol are deposited on carbon TEM grids. In both cases, the recorded images show almost spherical submicrometer-sized aggregates constituted by nanometer-sized crystals (Figures 2a and 2b). Parallel to that, similar observations performed on the ZnS and ZnS/PVP sols show very well defined single crystalline particles with a diameter of about 2 nm (Figures 2c and 2d).

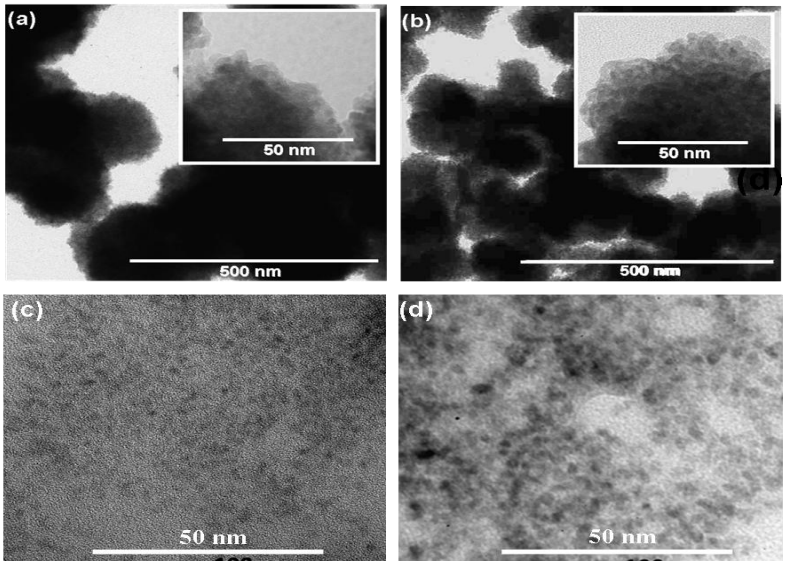

Figure 2. TEM images of the as-produced ZnS (a) and ZnS/PVP (b) powders and that of their respective DEG made sols (c) and (d). In each case, a zoom is given on inset to show the nanocrystalline character of the obtained powder.

Scanning electron microscopy image of the cross-section of the as-deposed ZnS/PVP film is given in the inset of Figure 1. It shows the formation of dense film with almost smooth surface. The thickness of the film is estimated to be about 2.5 μm. It shows that the subtract is uniformly covered by the film with the appearance of a certain number of cracks and pinholes.

3.2.Optical properties

Diffuse reflectance spectra of the ZnS powder (figure 3a) and ZnS/PVP powder (figure 3b) and film (figure 3f) were recorded in the UV-Visible spectral range and compared to that of commercial ZnS purchased from Fluka (Figures 3c).

The absorption spectra of ZnS and ZnS/PVP polyol-based sols were recorded in a transmission mode for comparison (Figure 3d and 3e). The energy gap of the powders and the film was determined by using the Kubelka-Munk function F(R) for the case of a direct band-to-band transition [26]. It corresponds to the intersection point of the extrapolated straight portion of the curve $(F(R).h\nu)^2$ vs. hν, the photon energy, with the abscissa axis (see the inset in Figure 3). That of the sols was directly inferred from the spectra. It corresponds to the intersection between the straight portion of the curve related to the gap absorption and the baseline. All the measured values are summarized in table 1. These are found to be almost similar in the sols and the films, significantly higher than that of the bulk (3.66 eV) in agreement with the expected quantum confinement effect related to the ultrafine crystal size (about 2 nm). The quantum confinement of both electrons and holes in semiconductors when their size is reduced to some nanometers leads to a band gap increase and then a size-related absorption edge blue shift, compared to the bulk [27]. Such a phenomenon is exactly observed when the radius of the semiconductor crystal is close or smaller than its Bohr radius (in the case of ZnS this radius is about 2.5 nm [28]). In the case of the ZnS/PVP powders, the larger crystal size (about 3 nm) leads to a lower absorption edge blue shift. Similar blue shift was reported by S. K. Panda et al., for submicrometer sized ZnS/PVP spheres constituted by ~3 nm sized semiconductor crystals [29]. They estimated the band gap of the samples produced by the precipitation route to 4.42 eV and used it as a probe that the ZnS nanocrystals can keep their individual properties in spite of their self assembly. In our case, this nanocrystal individual character is remarkably pronounced in the ZnS and ZnS/PVP sols and in the ZnS/PVP powder and film but slightly manifested in ZnS powder due to the strong aggregation state of its constitutive crystals (Table 1). Obviously, the experimental manifestation of the quantum confinement effect in semiconductors is the result of combined effects: i) their reduced size (QDs) and ii) their efficient dispersion in a transparent matrix (nanocomposites).

The efficiency of the dispersion in a nanocomposite can be indirectly evaluated by a comparison between the measured semiconductor crystal diameter and the calculated one (2R) considering the determined band gap blue shift through the following equation (Eq.1) [30,31].

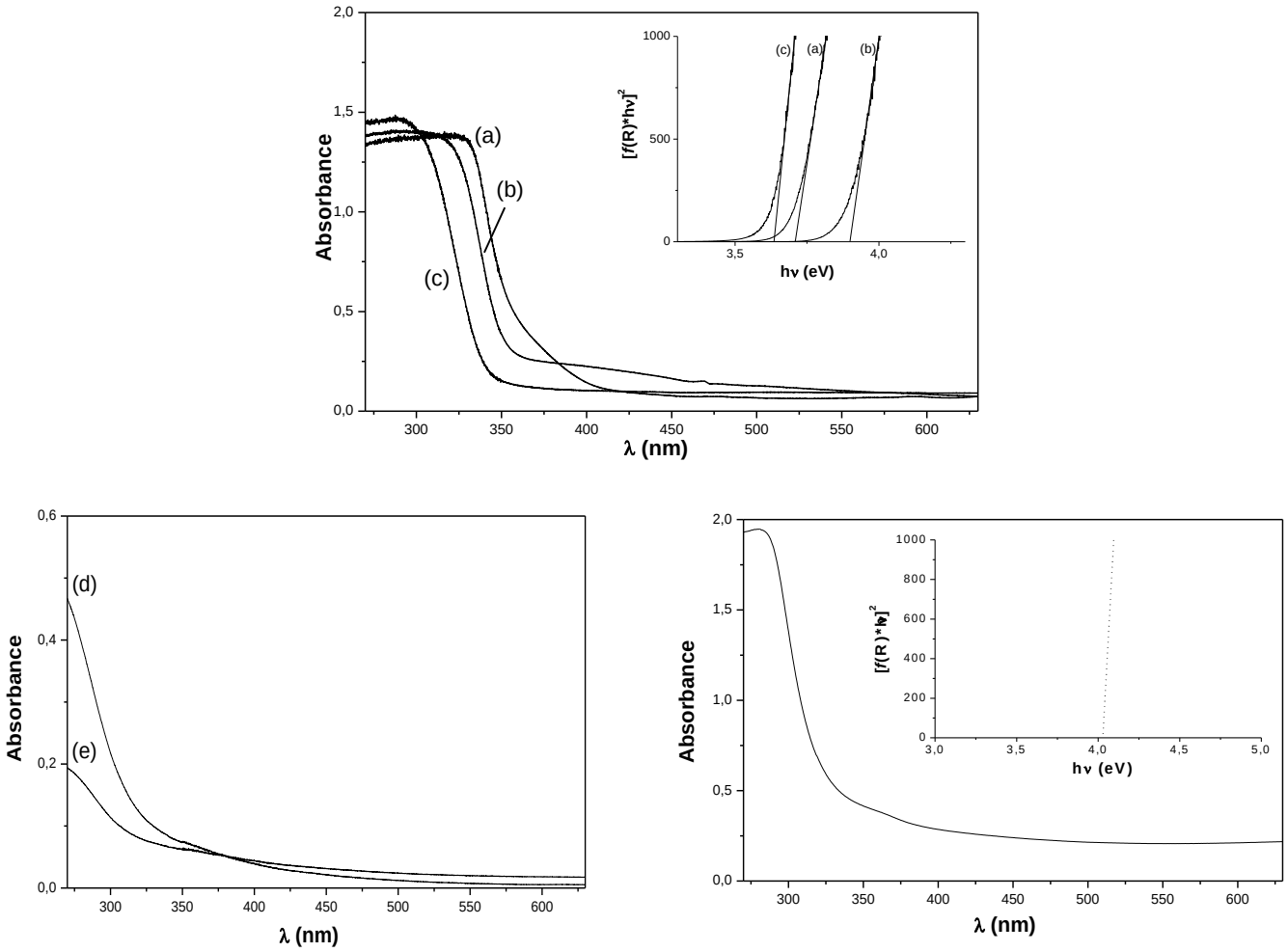

Figure 3. UV-Visible spectra of the as-produced ZnS (a) and ZnS/PVP (b) powders compared to those of bulk ZnS (c), polyol-based ZnS (d) and ZnS/PVP (e) sols and that of the ZnS/PVP film (f). Note that the a, b, c and f spectra were recorded in a diffuse reflectance mode while d and e ones were recorded in a transmission scheme. The corresponding Kubelka-Munk plots are given in the inset.

A great proximity between the two values should traduce a high level of dispersion of the crystals.

$$\Delta Eg = Eg(nano) - Eg(bulk) = (h^2/8\mu R^2) - (1.8e^2/\varepsilon R) \qquad (Eq.1)$$

where $\mu = m_e^* m_h^*/(m_e^* + m_h^*)$ corresponds to the reduced electron–hole effective mass (there are different estimations of the m_e^* and m_h^* constants leading to different μ values, varying from 0.13 to 0.31 according the assumed theoretical model [20,30,32,33]), ε is the dielectric constant of the bulk ZnS semiconductor, Eg(nano) and Eg(bulk) correspond to the band gap value of the nanomaterial and its bulk counterpart, respectively. The first term of Eq.1 traduces the confinement effect and the second one corresponds to the Coulomb interactions. When, the former is more important than the latter, Eq.1 can be summarized as follows:

$$\Delta Eg = Eg - Eg\ (bulk) = (h^2/8\mu R^2) \qquad (Eq.2)$$

In such a case, it becomes easy to calculate 2R (Table 1). Obviously, the calculated 2R values are close to the experimental ones for the sols and the nanocomposite powder and film and very far from that of the pure ZnS powder.

Conclusion

ZnS nanocrsytals have been successfully grown in a polyol medium in presence and absence of PVP chains. ZnS and ZnS/PVP sols and powders were successfully produced and the sols were used as spraying solution to produce composite film. As expected, the recorded XRD patterns, TEM images and UV-Visible diffuse reflectance spectra of the powders and film confirmed the formation of strongly aggregated blende-type ZnS

nanocrystals in absence of PVP and well dispersed ones in presence of PVP. The ZnS band gap increase due to the quantum confinement effect was enhanced in the nanocomposite materials than in the pure ones. Moreover, the characterized microstructre of the produced composite films (dense, continuous, smooth, thin…) show that the used here polyol-based sol spraying method is a very efficient and cheap route to produce ZnS/PVP films. These films have potential use in opto-electronic devices.

References

1. Xie W., Chen C., *Physica. B: Condens. Mater.*, 266 (1999) 373.
2. Tokio N., Keisuke F., Akio K., *IEEE Trans. Elect. Devices*, 46 (1999) 2093.
3. Falcony C., Garcia M., Ortiz A., Alonso. J.C., *J. Appl. Phys.*, 72 (1992) 1525.
4. Tang W., Cameron D.C., *Thin Solid Films*, 280 (1996) 221.
5. Ledger A. M., *Appl. Optic.*, 18 (1979) 2979.
6. Lu H.-Y., Chu S.-Y., Tan S.-S., *J. Cryst. Grow.*, 269 (2004) 385.
7. Murali K. R., Dhanemozhi A. C., John R., *J. All. Comp.*, 464 (2008) 383.
8. Feldmann C., Metzmacher C., *J.Mater. Chem.*, 11 (2001) 2603.
9. Zhao Y., Zhang Y., Zhu H., Hadjipanayis G. C., Xiao J. Q., *J. Am. Chem. Soc.*, 126 (2004) 6874.
10. Antoun T., Brayner R., Al Terary S., Fiévet F., Chehimi M., Yassar A., *Eur. J. Inorg. Chem.* (2007) 1275.
11. Ammar S., Helfen A., Jouini N., Fiévet F., Villain F., Rosenman I., Danot M., Molinié P., *J. Mater. Chem.*, 10 (2001) 186.
12. Chkaoundali S., Ammar S., Jouini N., Fiévet F., Richard M., Villain F., Grenèche J-M., Danot M., Molinié P., *J. Phys.: Condens. Mater.*, 16 (2004) 4357.
13. He Y., Wang J., *Mater. Lett.*, 62 (2008) 1379.
14. Li Y., Ding Y., Zhang Y., Qian Y., *J. Phys. Chem. Solids*, 60 (1999) 13.
15. Jiang C., Zhang W., Zou G., Yu W., Qian Y., *Mater. Chem. Phys.*, 103 (2007) 24.
16. Jayalakshmi M., Rao M. M., *J. Power Sources*, 157 (2006) 624.
17. Balá[ž]P., Boldi[ž]árová E., Godo[č]íková E., Brian[č]in J., *Mater. Lett.*, 57 (2003) 1585.
18. He R., X.- Yin F. Qian, J., Xi H.-A., L.-J. Zhu Bian, Z.-K., *Coll. Surf. A: Physicochem. Eng. Aspects*, 220 (2003) 151.
19. Wang L., Tao X.-T., Yang J.-X., Ren Y., Liu Z., Jiang M.-H., *Opt. Mater.*, 28 (2006) 1080.
20. Ghosh G., Kanti Naskar M., Patra A., Chatterjee M., *Opti. Mater.*, 28 (2006) 1047.
21. Maity R., Maiti U. N., Mitra M. K., Chattopadhyay K. K., *Physica E*, 33 (2006) 104.
22. Ullah M. H., Kim J.-H., Ha C.-S., *Mater. Lett.*, 62 (2008) 2249.
23. Beji Z., L. Smiri S., Vaulay M-J., Herbst F., Ammar S., Fiévet F., *Thin Solid Films*, 518 (2010) 2592.
24. Rodriguez-Carvajal J., computer program FULLPROF, Laboratoire Léon Brillouin CEA-CNRS, Grenoble, France, (1998).
25. Lutterotti L, Matthies S, Wenk HR. IUCr: *Newsletter of the Commission on Powder diffraction*, 21 (1999) 14.
26. Péré E., Cardy H., Cairon O., Simon M., Lacombe S., *Vibr. Spectr.*, 25 (2001) 163.
27. Murray C.B., Kagan C.R., Bawendi M.G., *Ann. Rev. Mater. Sci.*, 30 (2005) 345.
28. Wang C., Guan L., Mao Y., Gu Y., Liu J., Fu S., Xu Q., *J. Phys. D: Appl. Phys.*, 42 (2009) 045403.
29. Panda S. K., Datta A., Chaudhuri S., *Chem. Phys. Lett.*, 440 (2007) 235.
30. Sahraei R., Aval G.M., Goudarzi A., *J. All. Compds.*, 466 (2008) 488.
31. Woggon U., *Optical Properties of semiconductor quantum Dots, Springer, Berlin*, (1997).
32. Landolt-Bornstein, *Numerical data and functional relationship in science and technology, New Series*, 22, *Springer, Berlin*, (1987).
33. Kane E. O., Büttner P., *Phys. Rev.B*, 18 (1978) 6849.